# DECIPHERING METABOLIC ABNORMALITIES ASSOCIATED WITH ALZHEIMER'S DISEASE IN SERUM FROM THE APP/PS1 MOUSE MODEL USING INTEGRATED METABOLOMIC APPROACHES

Raúl González-Domínguez[a,b,c], Tamara García-Barrera[a,b,c], Javier Vitorica[d,e,f], José Luis Gómez-Ariza[a,b,c]

[a]Department of Chemistry and CC.MM. Faculty of Experimental Sciences. University of Huelva. Campus de El Carmen. 21007 Huelva. Spain; [b]Campus of Excellence International ceiA3. University of Huelva. Spain; [c]Research Center of Health and Environment (CYSMA). University of Huelva. Campus de El Carmen. 21007 Huelva. Spain; [d]Department Bioquímica, Bromatologia, Toxicología y Medicina Legal, Faculty of Pharmacy, University of Seville. 41012 Seville. Spain, [e]Centro de Investigación Biomédica en Red sobre Enfermedades Neurodegenerativas (CIBERNED). 41013 Seville. Spain, [f]Instituto de Biomedicina de Sevilla (IBiS)–Hospital Universitario Virgen del Rocío/CSIC/University of Seville. 41013 Seville. Spain

Corresponding authors:

Prof. J.L Gómez Ariza, Department of Chemistry and CC.MM. Faculty of Experimental Sciences. University of Huelva. Campus de El Carmen. 21007 Huelva. Spain. Tel.: +34 959 219968, fax: +34 959 219942, e-mail: ariza@uhu.es

Dr. T. Garcia-Barrera. Department of Chemistry and CC.MM. Faculty of Experimental Sciences. University of Huelva. Campus de El Carmen. 21007 Huelva. Spain. Tel.: +34 959 219962, fax: +34 959 219942, e-mail: tamara@dqcm.uhu.es

## ABSTRACT

The transgenic mouse APP/PS1 is widely employed by neuroscientists because reproduces well some of the neuropathological and cognitive deficits observed in human Alzheimer's disease. In this study, serum samples from APP/PS1 mice (n = 30) and wild-type controls (n = 30) were analyzed using a metabolomic multiplatform based on the combination of gas chromatography-mass spectrometry and ultra-high performance liquid chromatography-mass spectrometry, in order to obtain wide information about serum metabolome. Metabolic profiles showed significant differences between the groups of study, and numerous metabolites were identified as potential players in the development of Alzheimer-type disorders in this transgenic model. Pathway analysis revealed the involvement of multiple metabolic networks in the underlying pathology, such as deficiencies in energy metabolism, altered amino acid homeostasis, abnormal membrane lipid metabolism, and other impairments related to the integrity of the central nervous system. It is noteworthy that some of these metabolomic markers are in accordance with pathological alterations observed in human Alzheimer's disease, while others have not been previously described. Therefore, these results demonstrate the potential of metabolomics and the use of transgenic animal models to understand the pathogenesis of Alzheimer's disease.

**KEYWORDS.** Metabolomics, APP/PS1 mice, Alzheimer's disease, serum

**ABBREVIATIONS.** AD: Alzheimer's disease; GC-MS: gas chromatography mass spectrometry; UHPLC-MS: ultra-high performance liquid chromatography mass spectrometry; TG: transgenic; WT: wild type; QC: quality control; PCA: principal component analysis; PLS-DA: partial least squares discriminant analysis; VIP: variable importance in the projection; HEPE: hydroxyl-eicosapentaenoic acid; LPC: lyso-phosphocholine; LPI: lyso-phosphoinositol; LPE: lyso-phosphoethanolamine; PI: phosphoinositol; PC: phosphocholine; PE: phosphoethanolamine; PPE: plasmenylethanolamine; PPC: plasmenylcholine; SM: sphingomyelin.

## 1. INTRODUCTION

Alzheimer's disease (AD), the most common neurodegenerative disorder worldwide, is characterized by an insidious onset and a progressive decline of cognitive functions. It is recognized that genetics plays an important role in AD, principally due to mutations in the genes of amyloid precursor protein (APP) and presenilin 1 and 2 (PS1 and PS2), which lead to the accumulation of Aβ peptides [1]. However, the exact etiology and pathogenesis of this disorder is not clear, given that its study is hindered by the complex underlying biochemistry, the long presymptomatic period, the inability to study microscopic morphological changes in tissues until the final stage of the disease and the variability of clinical expression of symptoms. Thereby, nowadays AD can only be detected at advanced stages of disease by exclusion of other pathologies based on clinical criteria defined by the NINCDS-ADRDA, and a definitive diagnosis is only made when there is histopathological confirmation [2]. Therefore, early preclinical detection has become a primary focus of AD research. Numerous transgenic mouse models that mimic the main features of Alzheimer's disease have been developed to better understand the pathogenic mechanism of neurodegeneration and to test potential therapies [3]. In most of these models, the transgenic animals over-express mutated forms of human amyloid precursor protein, developing amyloid plaques with aging predominantly in the hippocampus and cortex. However, it has been demonstrated that co-expression of mutated human presenilin 1 or presenilin 2 in the model accelerates amyloid deposition. In this sense, the double mutant transgenic line APP/PS1 has been widely used in neuroscience studies given that reproduce some of the neuropathological and cognitive deficits observed in AD, with a phenotype characterized by early amyloid deposits and behavioral deficits [4].

Metabolomics presents a high potential in health survey and biomarkers discovery, because changes in specific groups of metabolites may be sensitive to pathogenically relevant factors. Thus, metabolomic profiling is emerging as a powerful tool for the characterization of complex phenotypes affected by both genetic and environmental factors [5]. Particularly, metabolomics plays a prominent role in biomarker identification of multifunctional disorders such as Alzheimer's disease, in which many heterogeneous cellular processes are involved. Numerous studies have been performed to assess the pathophysiological status of transgenic animals by postmortem analysis of brain tissue samples [6-9]. However, the use of peripheral biofluids has been only scarcely considered, although the discovery of a well-established peripheral biomarker easily accessible is of primary importance when considering the prevalence of this disease [10]. Jiang et al. found significant differences in endogenous metabolites from serum of the senescence-accelerated mouse, suggesting perturbed glucose and lipid metabolisms, and attenuated protective function of inosine [11]. In other studies, the metabolic profiles of both brain and plasma of transgenic mice were characterized and compared to those of wild-type mice [12-13]. Lower levels of metabolites were found in plasma samples, and they fluctuate more between the two groups than brain metabolites. However, the statistical models built using plasma metabolite profiles were more accurate than brain tissue despite the smaller number of factors. Finally, metabolomics has been also applied to examine changes in urinary metabolites of transgenic AD mice, demonstrating the utility of a very simple and easily available sample in clinical laboratory as is urine for the search of potential biomarkers [14-15].

In the study presented here, serum samples from APP/PS1 transgenic mice were analyzed by a metabolomic multiplatform combining gas chromatography-mass spectrometry (GC-MS) and ultra-high performance liquid chromatography-mass spectrometry (UHPLC-MS). No single analytical technique covers the entire spectrum of the metabolome, so the application of combined LC-MS and GC-MS technologies is becoming the most relevant tool for biomarkers discovery due to their complementarity. Gas chromatography-mass spectrometry has been traditionally employed for the profiling of low molecular weight metabolites with high sensitivity, peak resolution and reproducibility [16]. On the other hand, reversed-phase ultra-high performance liquid chromatography-mass spectrometry has become the main workhorse in metabolomics due to its high resolution and sensitivity, fast analysis and good potential for biomarker identification, which provides efficient retention and separation of relatively nonpolar metabolites across a large molecular weight range [17]. Thus, the application of this global metabolomic approach using two complementary platforms allowed a broad analytical coverage of serum metabolites, from small polar metabolites to lipids. Then, multivariate statistical analysis was used to differentiate serum metabolomic profiles of APP/PS1 mice from wild-type controls, and to identify perturbations in biochemical pathways related to pathological processes.

## 2. MATERIAL AND METHODS

### 2.1. ANIMAL HANDLING

Transgenic APP/PS1 mice (C57BL/6 background) were generated as previously described by Jankowsky et al., expressing the Swedish mutation of APP together with PS1 deleted in exon 9 [18]. On the other hand, age-matched wild-type mice of the same genetic background (C57BL/6) were purchased from Charles River Laboratory for their use as controls. In this study, male and female animals at 6 months of age were used for experiments (TG: N=30, male/female 13/17; WT: N=30, male/female 15/15). Animals were acclimated for 3 days after reception in rooms with a 12-h light/dark cycle at 20-25 °C, with water and food available *ad libitum*. Then, mice were anesthetized by isoflurane inhalation and blood was extracted by cardiac puncture. Blood samples were immediately cooled and protected from light for 30 minutes to allow clot retraction, and then centrifuged at 3500 rpm for 10 minutes at 4ºC. Serum was aliquoted in Eppendorf tubes and frozen at -80°C until analysis. Animals were handled according to the directive 2010/63/EU stipulated by the European Community, and the study was approved by the Ethical Committee of University of Huelva.

### 2.2. SERUM SAMPLES PREPARATION

For the extraction of metabolites, 100 µL of serum were mixed with 400 µL of methanol/ethanol (50% v/v) and vortexed for 5 min. Then, samples were centrifuged at 4000 rpm for 10 min at 4°C, and the supernatant was transferred to another tube to be dried under nitrogen stream. Finally, the resulting residue was reconstituted with methanol/water (80:20 v/v) containing 0.1% formic acid. An aliquot of this extract (50 µl) was split for derivatization before GC-MS fingerprinting, and the rest of the sample was transferred to the injection vial for LC-MS analysis. Derivatization was carried out according to the two step methodology proposed by Begley et al [19]. For this, 50µl of extracts were dried under nitrogen stream and redissolved in 50 µL of 20 mg $mL^{-1}$ methoxyamine in pyridine for protection of carbonyl groups by methoximation. After briefly vortexing, samples were incubated at 80°C for 15 min in a water bath. Then silylation was performed by adding 50 µL of MSTFA (N-methyl-N-trimethylsilyl trifluoroacetamide) and incubating at 80°C for a further 15 min. Finally, extracts were centrifuged at 4000 rpm for one minute and supernatant was collected for analysis.

### 2.3. METABOLOMIC PROFILING BY GC-MS

Analyses were performed in a Trace GC ULTRA gas chromatograph coupled to an ion trap mass spectrometer detector ITQ 900 (Thermo Fisher Scientific), using a Factor Four capillary column VF-5MS 30m×0.25mm ID, with 0.25 µm of film thickness (Varian). The GC column temperature was set to 100ºC for 0.5 minutes, and programmed to reach 320ºC at a rate of 15ºC per minute. Finally, this temperature was maintained for other 2.8 minutes, being the total time of analysis 18 minutes. The injector temperature was kept at 280ºC, and helium was used as carrier gas at a constant flow rate of 1 ml $min^{-1}$. For mass spectrometry detection, ionization was carried out by electron ionization (EI) using a voltage of 70 eV, and the ion source temperature was set at 200ºC. Data were obtained acquiring full scan spectra in the m/z range 35-650. For analysis, 1 µl of sample was injected in splitless mode.

### 2.4. METABOLOMIC PROFILING BY UHPLC-MS

Serum was fingerprinted by ultra-high performance liquid chromatography (Accela LC system, Thermo Fisher Scientific) coupled to a quadrupole-time-of-flight mass spectrometry system equipped with electrospray source (QSTAR XL Hybrid system, Applied Biosystems). Chromatographic separations were performed in a reversed-phase column (Hypersil Gold C18, 2.1x50 mm, 1.9µm) thermostated at 50ºC, with an injection volume of 5µl. Solvents were delivered at a flow rate 0.5ml/min, using methanol (solvent A) and water (solvent B), both containing 10mM ammonium formate and 0.1% formic acid. The gradient elution program was: 0-1 min, 95% B; 2.5 min, 25% B; 8.5-10 min, 0% B; 10.1-12 min, 95% B. MS operated in positive and negative polarities, acquiring full scan spectra in the m/z range 50-1000 with 1.005 seconds scan time. The ion spray voltage (IS) was set at 5000V and -2500V, and high-purity nitrogen was used as curtain, nebulizer and heater gas at flow rates about 1.48 L $min^{-1}$, 1.56 L $min^{-1}$ and 6.25 L $min^{-1}$, respectively. The source temperature was fixed at 400ºC, with a declustering potential (DP) of 100V/-120V, and a focusing potential (FP) of ±350V. To acquire MS/MS spectra, nitrogen was used as collision gas.

### 2.5. DATA PROCESSING

Raw data was processed following the pipeline described by Katajamaa et al., which proceeds through multiple stages including feature detection, alignment of peaks and normalization [20]. For this purpose, we employed the freely available software XCMS, included in the R platform (http://www.r-project.org). UHPLC-MS files were converted into mzXML format using the msConvert tool (ProteoWizard), while GC-MS files were converted into netCDF using the Thermo File Converter tool (Thermo Fisher Scientific). Subsequently, data were extracted using the matchedFilter method. This algorithm slices data

into extracted ion chromatograms (XIC) on a fixed step size (default 0.1 m/z), and then each slice is filtered with matched filtration using a second-derivative Gaussian as the model peak shape [21]. This filtration requires the optimization of two parameters in order to extract the maximum information as possible according to the characteristics of data sets obtained, named signal/noise threshold and full width at half-maximum (fwhm). The S/N threshold was set at 2 for both analytical approaches, while the optimal fwhm value was 10 for UHPLC-MS and 3 for GC-MS data, considering that lower peak widths are usually obtained in gas chromatography. After peak extraction, grouping and retention time correction of peaks (alignment) was accomplished in three iterative cycles with descending bandwidth (bw) from 10 to 1 seconds in UHPLC-MS, and descending bw from 5 to 1 seconds for GC-MS. Then, imputation of missing values was performed by returning to the raw spectral data and integrating the areas of the missing peaks which are below the applied signal-to-noise ratio threshold, using the fillPeaks algorithm. For data normalization, the locally weighted scatter plot smoothing (LOESS) normalization method was used, which adjusts the local median of log fold changes of peak intensities between samples in the data set to be approximately zero across the whole peak intensity range [22]. Finally, data were submitted to logarithmic transformation, in order to stabilize the variance of results. The preprocessed data were then exported as a .csv file for further data analysis by multivariate procedures.

### 2.6. DATA ANALYSIS

Data were subjected to multivariate analysis by principal component analysis (PCA) and partial least squares discriminant analysis (PLS-DA) in order to compare metabolomic profiles obtained, using the SIMCA-P™ software (version 11.5, UMetrics AB, Umeå, Sweden). Before performing statistical analysis, data are usually scaled and transformed in order to minimize the technical variability between individual samples to extract the relevant biological information from these data sets [23]. For this, data was submitted to Pareto scaling, for reducing the relative importance of larger values, and logarithmic transformation, in order to approximate a normal distribution. Quality of the models was assessed by the $R^2$ and $Q^2$ values, supplied by the software, which provide information about the class separation and predictive power of the model, respectively. These parameters are ranged between 0 and 1, and they indicate the variance explained by the model for all the data analyzed ($R^2$) and this variance in a test set by cross-validation ($Q^2$). Finally, potential biomarkers were selected according to the Variable Importance in the Projection, or VIP (a weighted sum of squares of the PLS weight, which indicates the importance of the variable in the model), considering only variables with VIP values higher than 1.5, indicative of significant differences among groups. In addition, groups comparison was conducted by t-test using the STATISTICA 8.0 software (StatSoft, Tulsa, USA). Only p values below 0.05 were regarded as statistically significant.

### 2.7. IDENTIFICATION OF BIOMARKERS

Potential biomarkers detected by GC-MS were identified using the NIST Mass Spectral Library (version 08). Alternatively, identification of metabolites from UHPLC-MS profiling was made matching the experimental accurate mass and tandem mass spectra (MS/MS) with those available in metabolomic databases (HMDB, METLIN and LIPIDMAPS), using a mass accuracy of 30 ppm. Furthermore, the identity of lipids was confirmed based on characteristic fragmentation patterns. Choline-containing phospholipids were detected as protonated and sodiated ions in positive ion mode, while in negative polarity these lipids formed demethylated ions or formate adducts. On the other hand, more abundant ions for ethanolamine species were $[M+H]^+$ and $[M-H]^-$, in positive and negative modes respectively. Finally, phosphatidylinositols were detected in negative ion mode in form of deprotonated ions. Phosphatidylcholines (PCs) and lysophosphatidylcholines (LPCs) presented characteristic ions in positive ionization mode at m/z 184.07, 104.10 and 86.09, and two typical fragments due to the loss of trimethylamine (m/z 59) and phosphocholine (m/z 183 or 205, if the counterion is proton or sodium). In contrast, the product-ion spectra of ethanolamines were dominated by $[M+H-141]^+$ arising from elimination of the phosphoethanolamine moiety. Finally, in negative mode these distinctive signals were found at 168.04, 196.07 and 241.02, for choline, ethanolamine and inositol derived lipids, respectively. Furthermore, the fragmentation in the glycerol backbone and release of the fatty acyl substituents enabled the identification of individual species of phospholipids, as previously described [24]. For sphingomyelins, typical product ions appear at m/z 264 and 282 due to the fragmentation in the sphingosine moiety, and the cleavage of phosphocholine headgroup generates characteristic fragments at 184.07 and 168.04 m/z, in positive and negative modes respectively [25]. Acylcarnitines were confirmed based on characteristic fragments of 60.08 and 85.03 m/z [26]. Finally, fatty acid amides [27], eicosanoids [28] and sphingoid bases [29] were also confirmed with characteristic fragments described in the literature.

### 2.8. METABOLIC PATHWAY ANALYSIS

Metabolic pathway analysis was subsequently performed to identify and visualize the affected metabolic pathways in APP/PS1 mice on the basis of potential biomarkers detected by GC-MS and UHPLC-MS profiling. For this purpose, the MetPA web tool was employed (http://metpa.metabolomics.ca), which conducts pathway analysis through pathway enrichment analysis and pathway topological analysis [30]. In this work, we select the *Mus musculus* library and use the default 'Hypergeometric Test' and 'Relative-Betweenness Centrality' algorithms for pathway enrichment analysis and pathway topological analysis, respectively. In order to identify the most relevant pathways, the impact-value threshold calculated from pathway topology analysis was set to 0.1.

## 3. RESULTS

### 3.1. MULTIVARIATE DATA ANALYSIS

The metabolomic approach based on the combination of GC-MS and UHPLC-MS profiling was applied to serum samples from APP/PS1 and wild-type mice in order to determine changes in metabolites associated with neurodegenerative processes. Due to the high complexity of metabolomic profiles obtained, multivariate data analysis based on projection methods was employed for the interpretation of results. Projection methods are based on the conversion of a multidimensional data table into a low-dimensional model through reduction of the high number of variables to obtain new variables or components (combinations of the originals) that are able to explain the variability of results [31]. These models make possible to extract and display the systematic variation in the data, and allow visualizing outliers, groupings and trends between different groups of samples, so they have become the main workhorse in chemometrics for metabolomics. In this way, after raw data processing, Pareto scaling and logarithmic transformation, data was submitted to multivariate statistics in order to build predictive models for classification of samples. As a first exploratory step, principal component analysis (PCA) was applied for a preliminary evaluation of the quality of the data before the application of any supervised statistical analysis. This unsupervised method was not able to discriminate between groups (Fig. 1A-C), as previously reported in other metabolomic studies with AD transgenic mice [11,14], but showed a clustering of samples in the scores plot without significant outliers (tested by inspection of Hotelling $T^2$-range plots). Subsequently, partial least squares discriminant analysis (PLS-DA) was used in the same data set to sharpen the separation between groups. PLS-DA scores plots (Fig 1D-F) displayed a clear separation between transgenic (TG) and control (WT) mice. Furthermore, the statistics parameters confirmed the goodness of these models (GC-MS: $R^2$=0.991 $Q^2$=0.802; UHPLC-MS(+): $R^2$=0.985 $Q^2$=0.938; UHPLC-MS(-): $R^2$=0.995 $Q^2$=0.944).

### 3.2. SELECTION OF BIOMARKERS

After PLS-DA modeling, data was further analyzed to identify the significant metabolites that contributed to the separation of groups. For this purpose, statistically significant metabolites were selected by inspecting loadings plots from PLS-DA, considering only metabolites with VIP values higher than 1.5, as well as by t-test ($p \leq 0.05$). In Table 1 are listed the potential biomarkers identified by UHPLC-MS, their experimental mass and retention time, the ionization mode used for detection, the fold change (calculated by dividing the mean area for peaks in the APP/PS1 group by the mean area in the control group) and p value (data for individual lipids are presented in electronic Supplementary Material, Table S1). On the other hand, significant compounds identified by GC-MS are summarized in Table 2, including the retention time, the fold change and p value.

As can be observed, complementary results were obtained from both analytical techniques employed in this study. Metabolomic profiling by UHPLC-MS highlighted the importance of different classes of lipids in the development of features of Alzheimer's disease displayed by the APP/PS1 mice, including phospholipids and lysophospholipids, eicosanoids, sphingomyelins and sphingoid bases, bile acids, and others. Alternatively, GC-MS showed that a number of low molecular weight metabolites were significantly perturbed in this mouse model, such as amino acids, hexoses or organic acids. Therefore, these results demonstrated that a broad number of metabolites can be detected by this metabolomic multiplatform, which provides a comprehensive overview of serum metabolome.

### 3.3. METABOLIC PATHWAY ANALYSIS

Pathway analysis was then performed to identify the altered biochemical networks associated with the metabolic perturbations presented in Tables 1-2, in order to elucidate the underlying pathological mechanisms occurring in the APP/PS1 mice. To this end, the MetPA web tool combines pathway enrichment analysis and pathway topology analysis to identify the most relevant metabolic pathways involved in the conditions under study, using pathways downloaded from the KEGG database. Thereby,

the pathway impact is calculated as the sum of the importance measures of the matched metabolites normalized by the sum of the importance measures of all metabolites in each pathway [30]. Finally, results from this pathway analysis can be visualized as a graphical output representing the p value for each metabolic pathway (log-transformed) *vs.* the calculated pathway impact, where each node represents a metabolic pathway and its size indicates the importance of this pathway in response to Alzheimer's disease (Fig. 2A). In this way, pathway analysis revealed that the most disturbed pathways were the metabolism of amino acids such as phenylalanine (a); glycine, serine and threonine (c); tryptophan (d); and tyrosine (h); metabolism of lipids as glycerophospholipids (b); sphingolipids (g); and ether lipids (l); perturbed inositol phosphate metabolism (k); and alterations related to energy metabolism, including glyoxylate and dicarboxylate metabolism (e); starch and sucrose metabolism (f); glycolysis (i); and TCA cycle (j).

## 4. DISCUSSION

The APP/PS1 mouse model reproduces well some of the neuropathological and cognitive deficits observed in human Alzheimer, with a phenotype characterized by deposition of Aβ plaques starting from the age of four months, glial activation, and deficits in cognitive functions at the age of six months [4]. Furthermore, the study of the neurochemical profile and age-dependent metabolic changes exhibited by this transgenic line has demonstrated that these alterations precede cognitive dysfunctions [32], being very similar to those found in AD patients. Therefore, the use of this model may be of great help for the investigation of pathological mechanisms associated with Alzheimer's disease. Serum metabolomics based on mass spectrometry techniques, coupled to both gas chromatography and ultra-high performance liquid chromatography, revealed significant alterations in numerous metabolites. Furthermore, the application of metabolic pathway analysis allowed the identification of multiple abnormal processes underlying the pathology.

It is noteworthy the presence of characteristic metabolomic signatures indicating a severe energy impairment, with altered serum levels of metabolites such as glucose, glucose-6-phosphate, glycerol-3-phosphate, 1,3-bisphosphoglycerate, inorganic phosphate, lactate, β-hydroxybutyrate, citrate, malate, succinate, oleyl-carnitine, stearic acid and creatinine. The reduction of the cerebral metabolic rate for glucose and oxygen is one of the main features of Alzheimer's disease, demonstrated by *in vivo* imaging using positron emission tomography [33]. This hypometabolic situation, occurring as a consequence of multiple metabolic defects, is finally reflected in perturbed levels of energy-related metabolites. Lower blood levels of glucose (Table 2) have been previously reported for different transgenic models of Alzheimer's disease [11-13], which suggests a change in carbohydrate and energy metabolism. In addition, the decrease observed in glycolytic intermediates such as glucose-6-phosphate and 1,3-bisphosphoglycerate, and the increase of glycerol-3-phosphate, precursor of glyceraldehydede-3-phosphate, also support an important dysfunction in glycolysis. In this sense, numerous alterations have been found in key glycolytic enzymes in AD, including increased glucose-6-phosphate dehydrogenase activity [34] and decreased glyceraldehyde-3-phosphate dehydrogenase activity [35], which is in agreement with our metabolomic findings. Serum concentration of inorganic phosphate is a determining factor in the regulation of energy metabolism and rate of oxygen consumption [36], so that reduced blood phosphate (Table 2) could be linked to a high demand by cells to stimulate metabolism of glucose. Mitochondrial dysfunction also plays a prominent role in energy deficiencies related to Alzheimer's disease. Significant impairments have been reported in multiple enzymes from the tricarboxylic acid cycle (TCA) [37], leading to abnormal levels of TCA intermediates and related compounds [38], in accordance with imbalances in serum concentrations of citrate, succinate and malate listed in Tables 1-2. In order to compensate these bioenergetic deficits caused by brain hypometabolism and impaired mitochondrial function, alternative pathways have been found significantly over-expressed in the APP/PS1 mice. The increase observed in serum lactate together with the reduction of glucose levels is consistent with a shift in energy metabolism toward anaerobic glycolysis. Under hypoxic conditions, neurons suffer adaptive processes to the reduced glucose consumption in order to maintain ATP levels, which are mediated by the hypoxia-inducible factor 1. This transcription factor induces the transcription of numerous genes related to hexoses metabolism including lactate dehydrogenase, but inhibits pyruvate dehydrogenase, thus promoting lactic fermentation instead of oxidative phosphorylation [39]. Thereby, a significant increase of lactate dehydrogenase activity has been previously found in AD brains, which produces an accumulation of lactate in brain [8,9,13] and blood [11,13]. Moreover, ketone body-driven energy production has been also proposed as a compensatory response when carbohydrate intake is low. Ketone bodies, principally acetoacetate and β-hydroxybutyrate, are produced from fatty acids in the liver and can be used to produce energy via conversion into acetyl-CoA and the TCA cycle. Yao et al. demonstrated that triple transgenic Alzheimer's mouse models use ketone bodies as alternative fuel to

sustain ATP generation, so that the decline in mitochondrial bioenergetics is accompanied by increased activity of 3-oxoacid-CoA transferase 1 (SCOT, required for ketone body utilization) [40]. This enhanced ketogenic pathway leads to decreased levels of ketone bodies such as β-hydroxybutyrate [13], in accordance with experimental data from GC-MS profiling in APP/PS1 mice (Table 2), and also supports the aforementioned increase in succinate levels, because it is a byproduct in the metabolism of ketone bodies by the action of SCOT. Another indicator of mitochondrial dysfunction observed in the APP/PS1 mice is the decrease of serum oleyl-carnitine and complementary increase of stearic acid levels. Lower levels of L-carnitine have been reported in AD [41-42], suggesting a perturbed transport of fatty acids into the mitochondria. Furthermore, different enzymes related to the β-oxidation pathway have been found over-expressed in AD, such as hydroxyacyl-coenzyme A dehydrogenase [40] or short chain 3-hydroxyacyl-CoA dehydrogenase [43]. Therefore, this impaired metabolism of lipids could be involved in neurodegenerative energetic failures as a supplementary pathway to those previously described. Finally, the increase in creatinine levels (Table 2) implies an abnormal metabolism of creatine in the APP/PS1 mice. Creatine plays a fundamental role in energy buffering and overall cellular bioenergetics by means of the creatine kinase/phosphocreatine system, being responsible for the transfer of energy from mitochondria to cytosol. Oxidative stress have been previously related to reduced creatine kinase activity in brain of AD patients, which finally results in reduced levels of creatine [41,42,44]. By contrast, levels of creatinine, the non-enzymatic degradation product of creatine and phosphocreatine, are usually higher in AD [9,42], which could indicate a dyshomeostasis of phosphocreatine system. Therefore, it could be concluded that deficits in bioenergetic metabolism is a key factor in pathogenesis of AD-type disorders found in the APP/PS1 mice, affecting multiple metabolic pathways such as glycolysis, TCA cycle, β-oxidation, ketogenic pathway and phosphocreatine system, as summarized in Figure 2B.

The decrease observed in adenosine monophosphate levels (Table 1) and the complementary increase of uric acid (Table 2) suggests an impaired purine metabolism. In this sense, Lin et al. found a perturbed catabolism of different purine derivatives toward the accumulation of uric acid in the cerebellum of transgenic CRND8 mice [45]. Moreover, the degradation of AMP may have important consequences in cellular energy homeostasis, since it plays a central role in glucose and lipid metabolism through the AMP-activated protein kinase, which is known to be decreased in AD brain [46]. Furthermore, the decrease of serum AMP levels could be related to an elevated adenosine monophosphate deaminase activity, which has been proposed as a potential source for ammonia production in Alzheimer's disease brain [47]. Hyperammonemia resulting from alterations in ammonia regulation, mainly due to urea cycle enzyme deficiencies, has deleterious effects on the central nervous system. In Alzheimer's disease, the alteration of urea cycle has been demonstrated on the basis of altered levels of expression in different enzymes and the corresponding genes [48]. Thus, abnormal content of urea and related amino acids has been previously reported in AD [44,49], in agreement with our metabolomic findings regarding reduced serum levels of urea and citrulline (Tables 1-2). Besides these metabolic alterations, other metabolites potentially involved in different pathways related to the integrity of the central nervous system were perturbed in serum from APP/PS1 mice, such as tyrosine, tryptophan, serotonin, fatty acid amides, monostearin and bile acids. Serotonin is a neurotransmitter derived from tryptophan involved in memory and learning, while tyrosine is the precursor of catecholamines such as dopamine or epinephrine. Thereby, reductions of serotonin, tryptophan and tyrosine levels denote a severe disturbance in monoaminergic neurotransmission systems, which confirm previous studies in AD subjects [41,44,50]. Fatty acid amides are a family of lipid signaling molecules that can act as regulators of several cellular and physiological functions, demonstrating control over a variety of biological processes such as sleep regulation, modulation of monoaminergic systems, locomotion, inhibition of phospholipase $A_2$ and epoxide hydrolase, among other processes [51]. These lipids are metabolized by the fatty acid amide hydrolase (FAAH), the principal catabolic enzyme of endocannabinoid system. The over-expression of FAAH has been previously associated with AD [52], which might lead to decreased levels of palmitamide and stearamide observed in serum of APP/PS1 mice (Table S1). On the other hand, the reduction of circulating levels of monostearin could be considered as an indicator of altered expression of monoacylglycerol lipase, also involved in endocannabinoid system and over-expressed in AD brain [53]. Therefore, reduced palmitamide, stearamide and monostearin could be considered as novel potential biomarkers of AD-type disorders in APP/PS1 mice indirectly related to endocannabinoid dysfunction, previously not described to our knowledge. Finally, decreased levels of deoxycholic, taurodeoxycholic and taurocholic acids were also observed in serum samples analyzed by UHPLC-MS (Table S1). In this context, ursodeoxycholic acid and tauroursodeoxycholic acid were demonstrated to be potent inhibitors of apoptosis [54], and they present neuroprotective action against amyloid deposition [55]. Therefore, although further studies have to be performed in order to confirm these results, these compounds

highlight as interesting potential markers of AD, especially considering their role as important metabolic integrators and signaling factors [56].

Numerous lipids also contributed significantly to discrimination between APP/PS1 mice and WT-controls considering the high impact-value calculated from pathway topology analysis (Fig. 2A), including choline, ethanolamine and inositol derived phospholipids and lyso-phospholipids, plasmalogens, sphingomyelins and sphingoid bases, as well as cholesterol, which may indicate an abnormal metabolism of membrane lipids. Membrane breakdown in AD has been traditionally related to over-activation of phospholipases, principally phospholipase $A_2$, leading to phospholipids degradation and resulting in the generation of second messengers involved in neurodegeneration [57]. However, this membrane destabilization process has been also associated with imbalance in the levels of saturated/unsaturated fatty acids contained in the structure of phospholipids [24,41]. In this study, decreased serum levels of different phospholipid species was observed, including cholines, ethanolamines, inositols and plasmalogens, most of them containing PUFAs in their structure, which is in accordance with previous studies in brain from transgenic mice of AD [6,7,58]. However, this is the first time that this finding is described in a peripheral sample as is serum. Furthermore, the release of fatty acids from the hydrolysis of these phospholipids by $PLA_2$ and subsequent oxidation supports the elevation of different eicosanoids in serum samples, such as prostaglandins (PG) and hydroxy-eicosapentaenoic acid (HEPE) (Table S1), which are important lipid mediators closely associated with neuronal pathways involved in AD neurobiology [59]. Moreover, lower concentrations of lyso-phospholipids were found in serum from APP/PS1 mice (Table S1), in agreement with previous studies in blood from human AD patients [24,29]. Therefore, results presented here demonstrate that phospholipids dyshomeostasis must be developed through similar pathways in both AD humans and transgenic mice. In addition, this altered metabolism of phospholipids in the APP/PS1 mice was also supported by other metabolomic changes in low molecular weight metabolites: phosphoethanolamine, myoinositol and myoinositol-1-phosphate. The decrease in phosphoethanolamine, the precursor of phosphatidylethanolamines, has been previously reported in postmortem AD brains [60], corroborating the evidence for a membrane defect in Alzheimer disease. On the other hand, perturbed levels of myoinositol and myoinositol-1-phosphate may be directly related to altered phosphatidylinositol metabolism and dysfunctions in the phosphoinositide signaling system. In this sense, previous reports have described increased levels of several isoenzymes of phosphoinositide-specific phospholipase C [61], as well as higher activity of myo-inositol monophosphatase in AD brains [62]. Therefore, an altered cellular homeostasis of myoinositol and their phosphorylated forms occurs in neurons, leading to the accumulation of free myoinositol, a conventional marker of astrogliosis and neuronal death, and decrease of myoinositol-1 phosphate in brains from both humans and animal models of AD [33,60].

Sphingolipid metabolism also seems to play a major role in the dysfunctional management of cellular membranes in the APP/PS1 mice, as can be observed in Table S1 considering reduced levels of different species of sphingomyelins and sphingoid bases. In Alzheimer's disease, perturbed sphingomyelin metabolism has been proposed as a pivotal event in the dysfunction and degeneration of neurons, with increased SM levels in CSF [63] and decreased in blood [64], while results from post-mortem brain analyses are contradictory, showing increased [58] or decreased [65] total concentrations of sphingomyelins. On the other hand, lipidomic investigations in transgenic mouse brains showed consistent increases of SM levels [58,66], but this is the first time that altered circulating levels of sphingomyelins in serum samples is observed. Moreover, decreased levels of sphinganine, hexadecasphinganine and phytosphingosine also support a disturbed sphingolipid metabolism, as previously reported in human serum [29]. Cholesterol is also an essential constituent of lipid rafts, whose reduction in brain can produce serious alterations of the physicochemical structure of lipid raft microdomains [66]. However, elevated blood levels of cholesterol and other lipids have been proposed to increase the risk of developing AD [67], as observed in our study (Table 2). Hyperlipidemia is one of the most important vascular risk factors, which can affect to cerebrovascular system causing atrophy, structural changes in the blood-brain barrier and inflammation. In this way, it is recognized that subjects with vascular risk factors have an increased prevalence of both vascular dementia and Alzheimer's disease [68], caused by decreased cerebral blood flow that finally involves neuronal cell loss.

Finally, decreased levels of amino acids glycine, threonine, proline and pyroglutamate were found by GC-MS profiling of serum samples (Table 2). By contrast, previous studies reported increased concentrations of several amino acids in brains from AD transgenic mice, including serine, threonine, valine, alanine, lysisne and leucine [7,8,9,12], which could indicate an important deregulation of the transport of amino acids across the blood brain barrier. Amino acids enter into the central nervous system by means of the sodium-independent system L1, which is regulated by the γ-glutamyl cycle [69]. In this process, amino

acids react with glutathione by the action of γ-glutamyl transpeptidase to form γ-glutamyl amino acids, which after enter cells are degraded to the corresponding amino acid, being liberated a molecule of pyroglutamate that is essential since stimulates sodium dependent carriers for the later removal of deleterious amino acids from brain. Changes in this cycle are known in AD brain, with a decrease of the GSH/GSSG ratio, diminished γ-glutamylcysteine synthetase activity and increased activity of enzymes related to the GSH use such as glutathione peroxidase, γ-glutamyl transpeptidase, and glutathione S-transferase [70]. In addition, reduced levels of pyroglutamate have been previously reported in AD brain [9], in accordance with our metabolomic results. Therefore, these data may suggest that disturbances in amino acids homeostasis play a critical role in the pathogenesis of AD in APP/PS1 mice.

## 5. CONCLUSIONS

In the present study, the APP/PS1 transgenic mice of Alzheimer's disease could be clearly differentiated from wild-type controls by metabolomic analysis of serum samples using combined GC-MS and UHPLC-MS. Subsequent application of metabolic pathway analysis allowed the elucidation of underlying pathological mechanisms occurring in the APP/PS1 mice, including failures in energy metabolism, perturbed homeostasis of membrane lipids and amino acids, as well as abnormal processes related to the integrity of the central nervous system, such as hyperammonemia, endocannabinoid dysfunction or monoaminergic alterations. Therefore, these findings stand out the potential of the APP/PS1 transgenic mice to study the pathogenesis and development of Alzheimer's disease, because many of these findings agree with pathological alterations observed in diseased humans.

**Acknowledgements.** This work was supported by the projects CTM2012-38720-C03-01 from the Ministerio de Ciencia e Innovación and P008-FQM-3554 and P009-FQM-4659 from the Consejería de Innovación, Ciencia y Empresa (Junta de Andalucía). Raúl González Domínguez thanks the Ministerio de Educación for a predoctoral scholarship.

## REFERENCES

[1] Bettens K, Sleegers K, Van Broeckhoven C. Genetic insights in Alzheimer's disease. Lancet Neurol 2013;2:92-104.

[2] McKahnn G, Drachman D, Folstein M, Katzman R, Price D, Stadlan EM. Clinical diagnosis of Alzheimer´s disease: report of the NINCDS-ADRDA Work Group under the auspices of Department of Health and Human Services Task Force on Alzheimer´s disease. Neurology 1984;34:939-44.

[3] Hall AM, Roberson ED. Mouse models of Alzheimer's disease. Brain Res Bull 2012;88:3-12.

[4] Malm T, Koistinaho J, Kanninen K. Utilization of APPswe/PS1dE9 transgenic mice in research of Alzheimer's disease: Focus on gene therapy and cell-based therapy applications. Int J Alzheimers Dis 2011;2011:517160.

[5] Lindon JC, Holmes E, Nicholson JK. Metabonomics and its role in drug development and disease diagnosis. Expert Rev Mol Diagn 2004;4:189-99.

[6] González-Domínguez R, García-Barrera T, Vitorica J, Gómez-Ariza JL. Region-specific metabolic alterations in brain of the APP/PS1 transgenic mice of Alzheimer's disease. Biochim Biophys Acta Mol Basis Dis 2014; 1842:2395-402.

[7] González-Domínguez R, García-Barrera T, Vitorica J, Gómez-Ariza JL. Metabolomic screening of regional brain alterations in the APP/PS1transgenic model of Alzheimer's disease by direct infusion mass spectrometry. J Pharm Biomed Anal 2015;102:425-35.

[8] Salek RM, Xia J, Innes A, Sweatman BC, Adalbert R, Randle S, McGowan E, Emson PC, Griffin JL. A metabolomic study of the CRND8 transgenic mouse model of Alzheimer's disease. Neurochem Int 2010;56:937-43.

[9] Trushina E, Nemutlu E, Zhang S, ChristensenT, Camp J, Mesa J, Siddiqui A, Tamura Y, Sesaki H, Wengenack TM, Dzeja PP, Poduslo JF. Defects in mitochondrial dynamics and metabolomic signatures of evolving energetic stress in mouse models of familial Alzheimer's disease. PLoS ONE 2012;7:e32737.

[10] Patel S, Shah RJ, Coleman P, Sabbagh M. Potential peripheral biomarkers for the diagnosis of Alzheimer's disease. Int. J. Alzheimers Dis 2011;2011:572495.

[11] Jiang N, Yan X, Zhou W, Zhang Q, Chen H, Zhang Y, Zhang X. NMR-based metabonomic investigations into the metabolic profile of the senescence-accelerated mouse. J Proteome Res 2008;7:3678-86.

[12] Hu ZP, Browne ER, Liu T, Angel TE, Ho PC, Chan ECY. Metabonomic profiling of TASTPM transgenic alzheimer's disease mouse model. J Proteome Res 2012;11:5903-13.

[13] Graham SF, Holscher C, McClean P, Elliott CT, Green BD. $^{1}$H NMR metabolomics investigation of an Alzheimer's disease (AD) mouse model pinpoints important biochemical disturbances in brain and plasma. Metabolomics 2013;9:974-83.

[14] Fukuhara K, Ohno A, Ota Y, Senoo Y, Maekawa K, Okuda H, Kurihara M, Okuno A, Niida S, Saito Y, Takikawa O. NMR-based metabolomics of urine in a mouse model of Alzheimer's disease: identification of oxidative stress biomarkers. J Clin Biochem Nutr 2013;52:133-8.
[15] Gonzalez-Dominguez R, Castilla-Quintero R, Garcia-Barrera T, Gomez-Ariza JL. Development of a metabolomic approach based on urine samples and direct infusion mass spectrometry. Anal Biochem 2014;465:20-7.
[16] Pasikanti KK, Ho PC, Chan ECY. Gas chromatography/mass spectrometry in metabolic profiling of biological fluids. J Chromatogr B Analyt Technol Biomed Life Sci 2008;871:202-11.
[17] Wilson ID, Nicholson JK,Castro-Perez J, Granger JH, Johnson KA, Smith BW, Plumb RS. High resolution "ultra performance" liquid chromatography coupled to oa-TOF mass spectrometry as a tool for differential metabolic pathway profiling in functional genomic studies. J Proteome Res 2005;4:591-8.
[18] Jankowsky JL, Fadale DJ, Anderson J, Xu GM, Gonzales V, Jenkins NA, Copeland NG, Lee MK, Younkin LH, Wagner SL, Younkin SG, Borchelt DR. Mutant presenilins specifically elevate the levels of the 42 residue beta-amyloid peptide in vivo: evidence for augmentation of a 42-specific g secretase. Hum Mol Genet 2004;13:159-70.
[19] Begley P, Francis-McIntyre S, Dunn WB, Broadhurst DI, Halsall A, Tseng A, Knowles J, HUSERMET Consortium, Goodacre R, Kell DB. Development and performance of a gas chromatography-time-of-flight mass spectrometry analysis for large-scale nontargeted metabolomic studies of human serum. Anal Chem 2009;81:7038-46.
[20] Katajamaa M, Oresic M. Data processing for mass spectrometry-based metabolomics. J Chromatogr A 2007;1158:318-28.
[21] Smith CA, Want EJ, O'Maille G, Abagyan R, Siuzdak G. XCMS: Processing mass spectrometry data for metabolite profiling using nonlinear peak alignment, matching, and identification. Anal Chem 2006;78:779-87.
[22] Veselkov KA, Vingara LK, Masson P, Robinette SL, Want E, Li JV, Barton RH, Boursier-Neyret C, Walther B, Ebbels TM, Pelczer I, Holmes E, Lindon JC, Nicholson JK. Optimized preprocessing of ultra-performance liquid chromatography/mass spectrometry urinary metabolic profiles for improved information recovery. Anal Chem 2011;83:5864-72.
[23] van den Berg RA, Hoefsloot HCJ, Westerhuis JA, Smilde AK, van der Werf MJ. Centering, scaling, and transformations: improving the biological information content of metabolomics data. BMC Genomics 2006;7:142.
[24] Gonzalez-Dominguez R, Garcia-Barrera T, Gomez-Ariza JL. Combination of metabolomic and phospholipid-profiling approaches for the study of Alzheimer's disease. J Proteomics 2014;104:37-47.
[25] Haynes CA, Allegood JC, Park H, Sullards MC. Sphingolipidomics: Methods for the comprehensive analysis of sphingolipids. J Chromatogr B Analyt Technol Biomed Life Sci 2009;877:2696-708.
[26] Vernez L, Hopfgartner G, Wenk M, Krahenbuhl S. Determination of carnitine and acylcarnitines in urine by high-performance liquid chromatography-electrospray ionization ion trap tandem mass spectrometry. J Chromatogr A 2003;984:203-13.
[27] Nichols KK, Ham BM, Nichols JJ, Ziegler C, Green-Church KB. Identification of fatty acids and fatty acid amides in human meibomian gland secretions. Invest Ophthalmol Vis Sci 2007;48:34-9.
[28] Murphy RC, Barkley RM, Berry KZ, Hankin J, Harrison K, Johnson C, Krank J, McAnoy A, Uhlson C, Zarini S. Electrospray ionization and tandem mass spectrometry of eicosanoids. Anal Biochem 2005;346:1-42.
[29] Li N, Liu W, Li W, Li S, Chen X, Bi K, He P. Plasma metabolic profiling of Alzheimer's disease by liquid chromatography/mass spectrometry. Clin Biochem 2010;43:992-7.
[30] Xia J, Wishart DS. MetPA: a web-based metabolomics tool for pathway analysis and visualization. Bioinformatics 2010;26:2342-4.
[31] Trygg J, Holmes E, Lundstedt T. Chemometrics in metabonomics. J Proteome Res 2007;6:469-79.
[32] Chen SQ, Cai Q, Shen YY, Wang PJ, Teng GJ, Zhang W, Zang FC. Age-related changes in brain metabolites and cognitive function in APP/PS1 transgenic mice. Behav Brain Res 2012;235:1-6.
[33] Ferreira IL, Resende R, Ferreiro E, Rego AC, Pereira CF. Multiple defects in energy metabolism in Alzheimer's disease. Curr Drug Targets 2010;11:1193-206.
[34] Russell RL, Siedlak SL, Raina AK, Bautista JM, Smith MA, Perry G. Increased neuronal glucose-6-phosphate dehydrogenase and sulfhydryl levels indicate reductive compensation to oxidative stress in Alzheimer disease. Arch Biochem Biophys 1999;370:236-9.
[35] Shalova IN, Cechalova K, Rehakova Z, Dimitrova P, Ognibene E, Caprioli A, Schmalhausen EV, Muronetz VI, Saso L. Decrease of dehydrogenase activity of cerebral glyceraldehyde-3-phosphate dehydrogenase in different animal models of Alzheimer's disease. Biochim Biophys Acta 2007;1770:826-32.

[36] Bose S, French S, Evans FJ, Balaban RS. Metabolic network control of oxidative phosphorylation: Multiple roles of inorganic phosphate. J Biol Chem 2003;278:39155-65.
[37] Bubber P, Haroutunian V, Fisch G, Blass JP, Gibson GE. Mitochondrial abnormalities in Alzheimer brain: mechanistic implications. Ann Neurol 2005;57:695-703.
[38] Redjems-Bennani N, Jeandel C, Lefebvre E, Blain H, Vidailhet M, Guéanta JL. Abnormal substrate levels that depend upon mitochondrial function in cerebrospinal fluid from Alzheimer patients. Gerontology 1998;44:300-4.
[39] Papandreou I, Cairns RA, Fontana L, Lim AL, Denko NC. HIF-1 mediates adaptation to hypoxia by actively down-regulating mitochondrial oxygen consumption. Cell Metab 2006;3:187-97.
[40] Yao J, Hamilton RT, Cadenas E, Brinton RD. Decline in mitochondrial bioenergetics and shift to ketogenic profile in brain during reproductive senescence. Biochim Biophys Acta 2010;1800:1121-6.
[41] González-Domínguez R, García-Barrera T, Gómez-Ariza JL. Using direct infusión mass spectrometry for serum metabolomics in Alzheimer's disease. Anal Bioanal Chem 2014;406:7137-48.
[42] González-Domínguez R, García A, García-Barrera T, Barbas C, Gómez-Ariza JL. Metabolomic profiling of serum in the progression of Alzheimer's disease by capillary electrophoresis-mass spectrometry. Electrophoresis 2014; 35:3321-30.
[43] Yang SY, He XY, Schulz H. 3-Hydroxyacyl-CoA dehydrogenase and short chain 3-hydroxyacyl-CoA dehydrogenase in human health and disease. FEBS J 2005;272:4874-83.
[44] González-Domínguez R, Garcia-Barrera T, Gomez-Ariza JL. Application of a novel metabolomic approach based on atmospheric pressure photoionization mass spectrometry using flow injection analysis for the study of Alzheimer's disease. Talanta 2015;131:480-9.
[45] Lin S, Kanawati B, Liu L, Witting M, Li M, Huang J, Schmitt-Kopplin P, Cai Z. Ultra high resolution mass spectrometry-based metabolic characterization reveals cerebellum as a disturbed region in two animal models. Talanta 2014;118:45-53.
[46] Cai Z, Yan LJ, Li K, Quazi SH, Zhao B. Roles of AMP-activated protein kinase in Alzheimer's disease. Neuromol Med 2012;14:1-14.
[47] Sims B, Powers RE, Sabina RL, Theibert AB. Elevated adenosine monophosphate deaminase activity in Alzheimer's disease brain. Neurobiol Aging 1998;19:385-91.
[48] Hansmannel F, Sillaire A, Kamboh MI, Lendon C, Pasquier F, Hannequin D, Laumet G, Mounier A, Ayral AM, DeKosky ST, Hauw JJ, Berr C, Mann D, Amouyel P, Campion D, Lambert JC. Is the urea cycle involved in Alzheimer's disease? J Alzheimers Dis 2010;21:1013-21.
[49] González-Domínguez R, García-Barrera T, Gómez-Ariza JL. Metabolomic study of lipids in serum for biomarker discovery in Alzheimer's disease using direct infusion mass spectrometry. J Pharm Biomed Anal 2014;98:321-6.
[50] Storga D, Vrecko K, Birkmayer JGD, Reibnegger G. Monoaminergic neurotransmitters, their precursors and metabolites in brains of Alzheimer patients. Neurosci Lett 1996;203:29-32.
[51] Ezzili C, Otrubova K, Boger DL. Fatty acid amide signaling molecules. Bioorg Med Chem Lett 2010;20:5959-68.
[52] Benito C, Nuñez E, Tolon RM, Carrier EJ, Rabano A, Hillard CJ, Romero J. Cannabinoid CB2 receptors and fatty acid amide hydrolase are selectively overexpressed in neuritic plaque-associated glia in Alzheimer's disease brains. J Neurosci 2003;23:11136-41.
[53] Mulder J, Zilberter M, Pasquaré SJ, Alpár A, Schulte G, Ferreira SG, Köfalvi A, Martín-Moreno AM, Keimpema E, Tanila H, Watanabe M, Mackie K, Hortobágyi T, de Ceballos ML, Harkany T. Molecular reorganization of endocannabinoid signalling in Alzheimer's disease. Brain 2011;134:1041-60.
[54] Ramalho RM, Viana RJS, Low WC, Steer CJ, Rodrigues CMP. Bile acids and apoptosis modulation: an emerging role in experimental Alzheimer's disease. Trends Mol Med 2008;14:54-62.
[55] Lo AC, Callaerts-Vegh Z, Nunes AF, Rodrigues CMP, D'Hooge R. Tauroursodeoxycholic acid (TUDCA) supplementation prevents cognitive impairment and amyloid deposition in APP/PS1 mice. Neurobiol Dis 2013;50:21-9.
[56] Thomas C, Pellicciari R, Pruzanski M, Auwerx J, Schoonjans K. Targeting bile-acid signalling for metabolic diseases. Nat Rev Drug Discov 2008;7:678-93.
[57] Farooqui AA, Ong WY, Horrocks LA. Biochemical aspects of neurodegeneration in human brain: involvement of neural membrane phospholipids and phospholipases $A_2$. Neurochem Res 2004;29:1961-77.
[58] Chan RB, Oliveira TG, Cortes EP, Honig LS, Duff KE, Small SA, Wenk MR, Shui G, Di Paolo G. Comparative lipidomic analysis of mouse and human brain with Alzheimer disease. J Biol Chem 2012;287:2678-88.
[59] Frisardi V, Panza F, Seripa D, Farooqui T, Farooqui AA. Glycerophospholipids and glycerophospholipid-derived lipid mediators: A complex meshwork in Alzheimer's disease pathology. Prog Lipid Res 2011;50:313-30.

[60] Klunk WE, Panchalingam K, McClure RJ, Stanley JA, Pettegrew JW. Quantitative $^{1}H$ and $^{31}P$ MRS of PCA extracts of postmortem Alzheimer's disease brain. Neurobiol Aging 1996;17:349-57.
[61] Shimohama S, Sasaki Y, Fujimoto S, Kamiya S, Taniguchi T, Takenawa T, Kimura J. Phospholipase C isoenzymes in the human brain and their changes in Alzheimer's disease. Neuroscience 1998;82:999-1007.
[62] Shimohama S, Tanino H, Sumida Y, Tsuda J, Fujimoto S. Alteration of myo-inositol monophosphatase in Alzheimer's disease brains. Neurosci Lett 1998;245:159-62.
[63] Kosicek M, Zetterberg H, Andreasen N, Peter-Katalinic J, Hecimovic S. Elevated cerebrospinal fluid sphingomyelin levels in prodromal Alzheimer's disease. Neurosci Lett 2012;516:302-305.
[64] Han X, Rozen S, Boyle SH, Hellegers C, Cheng H, Burke JR, Welsh-Bohmer KA, Doraiswamy PM, Kaddurah-Daouk R. Metabolomics in early Alzheimer's disease: identification of altered plasma sphingolipidome using shotgun lipidomics. PLoS ONE 2011;6:e21643.
[65] Cutler RG, Kelly J, Storie K, Pedersen WA, Tammara A, Hatanpaa K, Troncoso JC, Mattson MP. Involvement of oxidative stress-induced abnormalities in ceramide and cholesterol metabolism in brain aging and Alzheimer's disease. Proc Natl Acad Sci 2004;101:2070-5.
[66] Fabelo N, Martín V, Marín R, Santpere G, Aso E, Ferrer I, Díaz M. Evidence for premature lipid raft aging in APP/PS1 double-transgenic mice, a model of familial Alzheimer disease. J Neuropathol Exp Neurol 2012;71:868-81.
[67] Pappolla MA, Bryant-Thomas TK, Herbert D, Pacheco J, Fabra Garcia M, Manjon M, Girones X, Henry TL, Matsubara E, Zambon D, Wolozin B, Sano M, Cruz-Sanchez FF, Thal LJ, Petanceska SS, Refolo LM.Mild hypercholesterolemia is an early risk factor for the development of Alzheimer amyloid pathology. Neurology 2003;61:199-205.
[68] Breteler MMB. Vascular risk factors for Alzheimer's disease: An epidemiologic perspective. Neurobiol Aging 2000;21:153-60.
[69] Lee WJ, Hawkins RA, Peterson DR, Viña JR. Role of oxoproline in the regulation of neutral amino acid transport across the blood-brain barrier. J Biol Chem 1996;271:19129-33.
[70] Zhu Y, Carvey PM, Ling Z. Age-related changes in glutathione and glutathione-related enzymes in rat brain. Brain Res 2006;1090:35-44.

**FIGURE LEGENDS**

**Fig 1.** Scores plots of PCA (A-C) and PLS-DA (D-F) models for GC-MS, UHPLC-ESI(+)/MS and UHPLC-ESI(-)/MS data

**Fig 2.** (A) Pathway analysis overview showing altered metabolic pathways in serum from APP/PS1 mice. (a) phenylalanine metabolism; (b) glycerophospholipid metabolism; (c) glycine, serine and threonine metabolism; (d) tryptophan metabolism; (e) glyoxylate and dicarboxylate metabolism; (f) starch and sucrose metabolism; (g) sphingolipid metabolism; (h) tyrosine metabolism; (i) glycolysis; (j) TCA cycle; (k) inositol phosphate metabolism; (l) ether lipids metabolism. (B) Overview of serum metabolomic changes in APP/PS1 mice related to bioenergetic metabolism; (↑) increased; (↓) decreased. Abbreviations: Glc, glucose; Glc-6-P, glucose-6-phosphate; G-3-P, glycerol-3-phosphate; 1,3-BPG, 1,3 bisphosphoglycerate; Pi, inorganic phosphate; βHB, β-hydroxybutyrate.

**Table 1.** Potential biomarkers identified by UHPLC-MS profiling of serum samples

| metabolite | mass (Da) | RT (min) | ion mode | fold change | p value |
|---|---|---|---|---|---|
| Phosphoethanolamine | 141.022 | 0.30 | P | 0.83 | 0.0196 |
| Adenosine monophosphate | 347.056 | 0.30 | P | 0.61 | 0.0016 |
| Citrulline | 175.101 | 0.30 | N | 0.80 | 0.0021 |
| Citric acid | 192.031 | 0.35 | N | 0.66 | 0.0044 |
| C18:1-carnitine | 425.341 | 4.77 | P | 0.94 | 0.0439 |
| Monostearin | 358.291 | 5.67 | P | 0.70 | 0.0475 |
| Bile acids | Table S1 | | | ↓ | - |
| Eicosanoids | Table S1 | | | ↑ | - |
| Fatty acid amides | Table S1 | | | ↓ | - |
| Sphingoid bases | Table S1 | | | ↓ | - |
| Lyso-phospholipids | Table S1 | | | ↓ | - |
| Phospholipids | Table S1 | | | ↓ | - |
| Sphingomyelins | Table S1 | | | ↓ | - |

*Abbreviations: P: positive mode, N: negative mode.*

**Table 2.** Potential biomarkers identified by GC-MS profiling of serum samples

| **metabolite** | **RT (min)** | **fold change** | **p value** |
|---|---|---|---|
| Lactic acid | 2.75 | 1.69 | 0.0249 |
| β-hydroxybutyric acid | 3.42 | 0.52 | 0.0427 |
| Urea | 4.13 | 0.50 | 0.0001 |
| Phosphoric acid | 4.25 | 0.89 | 0.0350 |
| Glycine | 4.47 | 0.41 | 0.0003 |
| Succinic acid | 4.53 | 3.35 | 0.0069 |
| Threonine | 5.05 | 0.65 | 0.0134 |
| Malic acid | 5.92 | 0.83 | 0.0481 |
| Pyroglutamic acid | 6.23 | 0.58 | 0.0357 |
| Creatinine | 6.55 | 1.87 | 0.0475 |
| Proline | 6.68 | 0.58 | 0.0436 |
| Glycerol-3-phosphate | 8.02 | 1.12 | 0.0464 |
| Citric acid | 8.45 | 0.57 | 0.0284 |
| Glucose | 8.87 | 0.51 | 0.0002 |
| Tyrosine | 9.35 | 0.73 | 0.0410 |
| Myoinositol | 10.25 | 1.14 | 0.0453 |
| Uric acid | 10.37 | 1.55 | 0.0448 |
| Glucose-6-phosphate | 11.02 | 0.91 | 0.0483 |
| Tryptophan | 11.15 | 0.62 | 0.0238 |
| Stearic acid | 11.28 | 1.11 | 0.0462 |
| Myoinositol-1-phosphate | 12.13 | 0.73 | 0.0372 |
| Serotonin | 12.52 | 0.43 | 0.0147 |
| 1,3 Bisphosphoglycerate | 15.55 | 0.67 | 0.0475 |
| Cholesterol | 16.45 | 1.19 | 0.0043 |

Fig 1

Click here to download high resolution image

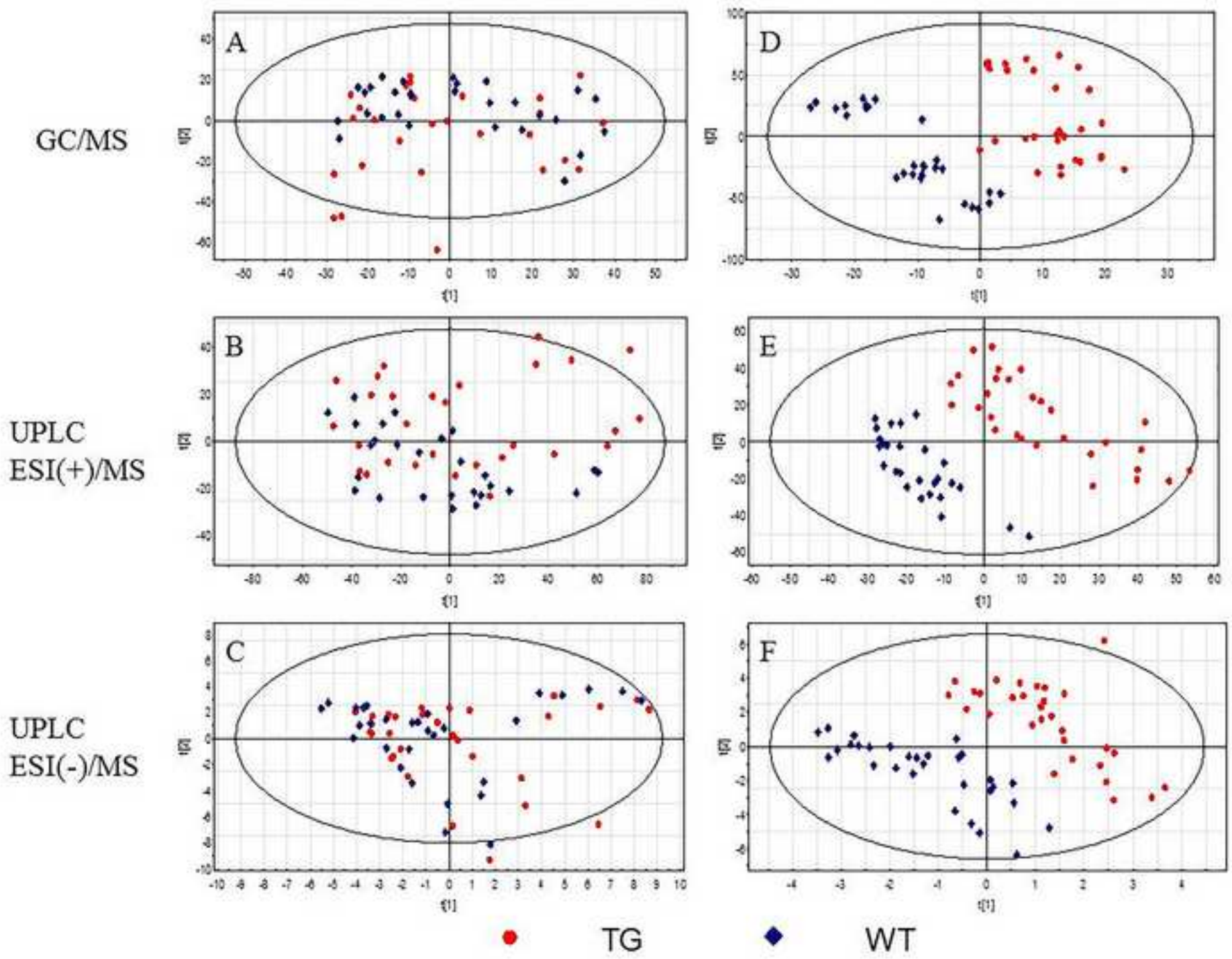

Fig 2

Click here to download high resolution image

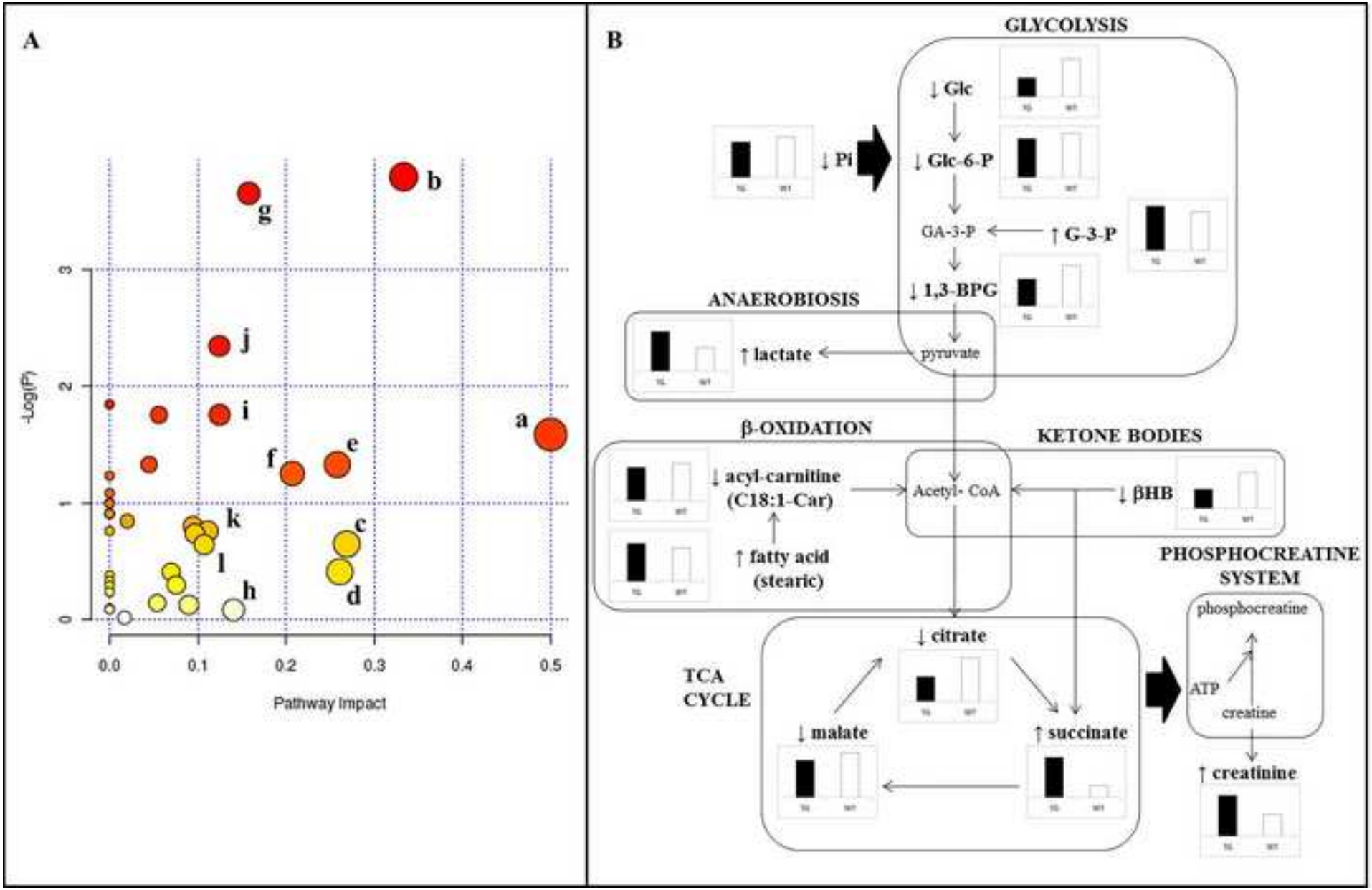

**Supplementary Material**

**Click here to download Supplementary Material: Supplementary material.docx**